Regular Paper:

An O-glycosyltransferase promotes cell adhesion during development by influencing secretion of an extracellular matrix integrin ligand

Liping Zhang, Duy T. Tran and Kelly G. Ten Hagen

J. Biol. Chem. *published online April 6, 2010*

JBC Papers in Press. Published on April 6, 2010 as Manuscript M109.098145
The latest version is at http://www.jbc.org/cgi/doi/10.1074/jbc.M109.098145

AN O-GLYCOSYLTRANSFERASE PROMOTES CELL ADHESION DURING DEVELOPMENT BY INFLUENCING SECRETION OF AN EXTRACELLULAR MATRIX INTEGRIN LIGAND

Liping Zhang[1], Duy T. Tran[1] and Kelly G. Ten Hagen[1, 2]

[1]Developmental Glycobiology Unit,
NIDCR, National Institutes of Health, Bethesda, Maryland 20892-4370

Running head: O-Glycosylation Affects ECM Composition

[2]Address correspondence to: Kelly G. Ten Hagen, Ph.D., Building 30, Room 426, 30 Convent Drive, MSC 4370, Bethesda, MD 20892-4370. Tel: 301-451-6318; Fax: 301-402-0897; Email: Kelly.Tenhagen@nih.gov

Protein secretion and localization are crucial during eukaryotic development, establishing local cell environments as well as mediating cell interactions, signaling and adhesion. In the present study, we demonstrate that the glycosyltransferase, *pgant3*, specifically modulates integrin-mediated cell adhesion by influencing the secretion and localization of the integrin ligand, tiggrin. We demonstrate that tiggrin is normally O-glycosylated and localized to the basal matrix where the dorsal and ventral cell layers adhere in wild type *Drosophila* wings. In *pgant3* mutants, tiggrin is no longer O-glycosylated and fails to be properly secreted to this basal cell layer interface, resulting in disruption of integrin-mediated cell adhesion in the wing. *pgant3*-mediated effects are dependent on enzymatic activity, as mutations that form a stable protein yet abrogate O-glycosyltransferase activity result in tiggrin accumulation within the dorsal and ventral cells comprising the wing. Our results provide the first in vivo evidence for the role of O-glycosylation in the secretion of specific extracellular matrix proteins, thus altering the composition of the cellular "microenvironment", and thereby modulating developmentally-regulated cell adhesion events. As alterations in cell adhesion are a hallmark of cancer progression, this work provides insight into the long-standing association between aberrant O-glycosylation and tumorigenesis.

Integrin-mediated adhesion is a crucial process involved in many aspects of development, tissue maintenance and disease. Integrin transmembrane receptors bind to extracellular matrix (ECM) ligands to coordinate cell-matrix and cell-cell adhesion as well as regulate cell morphology and signaling events (1-8). ECM ligands are a diverse group of molecules that are secreted by cells, creating local environments and matrices that modulate cell interactions. Mutations in integrins or their ECM ligands have been shown to disrupt cell adhesion, resulting in wing blistering (1,3-5,7,9-12), muscle detachment (3,13,14) and defects in dorsal closure (15) in *Drosophila*, as well as in the human disease epidermolysis bullosa, in which the epidermal and dermal skin layers are separated (16,17). Loss of proper cell adhesive properties is also a hallmark of cancer progression and metastasis.

We have previously shown that an ECM protein, tiggrin (3,18,19), is normally modified by the post-translational addition of the sugar N-acetylgalactosamine (GalNAc) (20) through the action of a member of the PGANT family of glycosyltranferases (EC 2.4.1.41). This type of evolutionarily conserved protein modification, known as mucin-type O-glycosylation (21-23), was shown to be required for proper cell

adhesion between the epithelial cell layers comprising the *Drosophila* wing blade. Loss of the gene encoding the enzyme responsible for glycosylating tiggrin (*pgant3*), resulted in the formation of wing blisters in adult flies (similar to those seen in homozygous *tiggrin* mutant escapers; 3), which could be rescued upon expression of wild type *pgant3* (20). Additionally, *pgant3* and *tiggrin* genetically interact to influence wing blistering frequency (20).

While loss of mucin-type O-glycosylation is associated with a number of diseases and developmental defects (22,24-30), the mechanistic role of mucin-type O-glycans in most of these instances remains unclear. Previous studies have suggested that O-glycans may influence protein stability, as is thought to be the case in the human disease, familial tumoral calcinosis (26,31-32). Other studies in cell culture using chemical inhibitors of O-glycan extension, have demonstrated that alterations in O-glycan formation can affect secretion and trafficking of certain proteins 33-36). However, these inhibitors also affect other glycosylation pathways, making specific conclusions about the role of mucin-type O-glycans difficult. In the present study, we demonstrate that mucin-type O-glycosylation promotes a developmentally-regulated cell adhesion event via influencing the proper secretion of an ECM component involved in integrin interactions. This study provides the first example of O-glycosylation influencing the composition of the extracellular matrix and suggests roles for this abundant protein modification in other developmental contexts as well as in disease states where matrix composition and cell adhesion are altered.

EXPERIMENTAL PROCEDURES

Fly strains used- The stocks used in this study are as follows: Bloomington stocks #3960 (if^3); #4533 (w^*; $In(2LR)no^{c4L}Sco^{rv9R}$, b^1/CyO, *P{ActGFP}JMR1*); and #7748 (w^{1118}; *Df(2R)Exel6283, P{XP-U}Exel6263*). Additionally, the following stocks from other sources were used: the w^*; $pgant3^{c01318}/pgant3^{c01318}$ transposon insertion line (20,37); the w^*; $pgant3^{hopout\#7}/pgant3^{hopout\#7}$ transposon excision line (20); and finally, the *w; Sco/SM6a* and $cn^1\ bw^1\ sp^1$ lines (the kind gifts of Dr. J. Kennison).

EMS mutagenesis screening and sequencing- Ethyl methane sulfonate (EMS) mutagenesis was carried out as described (38). Briefly, $cn^1\ bw^1\ sp^1$ males were fed EMS and crossed to the homozygous *pgant3* transposon insertion line, (w^*; $pgant3^{c01318}/pgant3^{c01318}$). From the F1 progeny, the individual males with blistered wings were collected and backcrossed to virgins from the homozygous *pgant3* transposon insertion line. F2 progeny displaying blistered wings were then collected and crossed to *w; Sco/SM6a* to make a balanced stock of the putative *pgant3* mutations.

Putative *pgant3* mutation lines were then crossed to a deficiency line ((*Df(2R)Exel6283, P{XP-U}Exel6263*) that uncovers *pgant3*. Heterozygous progeny from these crosses ($pgant3^{mutant}$/*Df(2R)Exel6283, P{XP-U}Exel6263*) were used for sequencing to verify that the new EMS-generated mutations were in the *pgant3* gene. Briefly, heterozygous adults were homogenized and RNA was isolated using the FastRNA Pro Green kit (Q-BIOgene). cDNA synthesis was performed using iScript cDNA Synthesis Kit (Bio-Rad). PCR primers were designed to yield four products covering the *pgant3* coding region: sense (GATCGGTTTGGATTGGATTG) and anti-sense (CGAGGCGGCACCACAACTG), to amplify the first exon and a portion of the second exon; sense (CCACTACATCGGCAAGGGAGAC) and anti-sense (ACCTTGCGTGATTCCTTAATGCG), to amplify part of the second exon, third exon,

fourth exon and a portion of the fifth exon; sense (GGCGATGTGCTGACCTTCCTC) and anti-sense (TTCATGTGCTTGCTGTAGGC) to amplify the first portion of the fifth exon; sense (GCCAAGGACAAGGTGAATGT) and anti-sense (ACCGGCATGACATGACATCCTACTC), to amplify the remainder of the fifth exon and the sixth exon. The resulting PCR fragments were purified using QIAquick Gel Extraction Kit (QIAGEN) and sequenced directly. From this analysis, two new *pgant3* mutations were identified and designated *pgant3*^{m1} and *pgant3*^{m2}. *pgant3*^{m1} *and pgant3*^{m2} stocks were then crossed to the previously described *pgant3* transposon insertion line and deletion line to determine wing blistering frequencies.

Expression and localization of PGANT3, PGANT3^{m1} *and PGANT3*^{m2} *enzymes in Drosophila cells*- cDNAs encoding *pgant3, pgant3*^{m1} *and pgant3*^{m2} were digested with EcoRI and NotI, and subcloned into pIB/V5-His vector (Invitrogen), to form a C-terminal V5 fusion. S2R+ cells were transfected with plasmids using Effectene transfection reagent (Qiagen) according to manufacturer's instructions. After 3 days, cells were fixed, stained with anti-V5 antibody (dilution 1:500) (Invitrogen) and the *Drosophila* Golgi marker GM130 (dilution, 1:100) (Abcam). After primary antibody staining, the cells were washed and incubated with Alexa 488 conjugated anti-mouse IgG secondary antibodies (dilution, 1:100) (Invitrogen) and Cy3-conjugated anti-rabbit IgG antibody (dilution, 1:100) (Jackson ImmunoResearch Laboratories).

Expression of secreted PGANT3, PGANT3^{m1} *and PGANT3*^{m2} *enzymes in COS7 cells*- The plasmids constructed above for localization studies of PGANT3 and PGANT3^{m2} were partially digested with AgeI to release fragments beginning just after the hydrophobic membrane spanning domain and ending after the V5 epitope at the C-terminus. These fragments were then subcloned into the vector pF4-FlyB (39) to generate constructs encoding secreted enzymes with a C-terminal V5 tag (pF4-pgant3-V5 and pF4-pgant3^{m2}-V5). For the *pgant3*^{m1} construct, sense (ATAACGCGTTCCAGGGCGGGGACGCGG AG) and anti-sense (GTGGCGCGGCGACCGGTTGATGAC) PCR primers were using to amplify a 435 bp *pgant3*^{m1} fragment beginning just after the hydrophobic region. The amplified PCR fragment was then digested with MluI and AgeI and cloned into the same sites of the vector pF4-pgant3-V5. All constructs were verified by DNA sequencing. Plasmids were transfected into COS7 cells using Lipofectamine reagent (Invitrogen). After 4 days, the media were harvested. To quantitate the relative amount of recombinant proteins secreted into the media, aliquots of media were electrophoresed under reducing conditions and transferred to nitrocellulose membranes. Membranes were incubated with anti-V5 antibody (dilution 1:2000) (Invitrogen) after blocking, and developed with HRP-conjugated mouse IgG (dilution 1:2000) (Cell Signaling Technology).

Glycosyltransferase assays- Assays for glycosyltransferase activity were performed as described previously (39). Briefly, media from COS7 cells expressing recombinant PGANT3 and PGANT3^{m1} were harvested and recombinant proteins were quantitated by western blotting as described above. Equal relative amounts of each recombinant protein were used in the in vitro reactions with sugar donor ^{14}C-UDP-GalNAc and various concentrations (62.5-250 μM) of the EA2 acceptor substrate (PTTDSTTPAPTTK). All reactions were performed in triplicate at 37^{o}C for 1 hr. Reaction products were purified by anion exchange chromatography and ^{14}C-GalNAc incorporation was measured. Reactions using media from cells expressing empty vector alone yielded background values that were subtracted

from each experimental value. Adjusted experimental values were then averaged and standard deviations were calculated. Glycosyltransferase activity is expressed as dpm/hr.

Pupal wing disc staining- Pupae were staged from pupariation (white prepupa). Staged pupae were immersed in 4% formaldehyde in PBS and then an incision was made through the pupal case and the body wall. Fixation was continued on a shaker for at least 1hr at room temperature (RT). Fixed pupae were then stored at 4°C. Pupal cases were removed and pupal wings were dissected. Samples were washed in PBST (PBS-0.3% Triton X-100) and transferred to blocking buffer (4% goat serum-PBS-0.3% Triton X-100) for 1hr on a shaker. Samples were then incubated with primary antibody overnight at 4°C in blocking buffer. Primary antibodies used were mouse anti-β-PS-integrin (40) (Developmental Studies Hybridoma Bank, 1:100), rat anti-DE-cadherin (40) (Developmental Studies Hybridoma Bank, 1:100), mouse anti-Fasciclin III (40) (Developmental Studies Hybridoma Bank, 1:100), mouse anti-tiggrin antibody (18) (the kind gift of Drs. L. and J. Fessler, 1:100), mouse anti-Tn antibody (Ca3638) (41) (the kind gift of Dr. Richard Cummings, 1:50). Alexa 488-, 568- and 647-conjugated secondary antibodies (Invitrogen, 1:100) and Cy3-conjugated donkey anti-mouse IgM antibody (Jackson ImmunoResearch Laboratories, 1:100) were used. Nuclei were stained with 4',6-diamidino-2-phenylindole, dihydrochloride (DAPI) (Sigma, 1:1000). Wings were mounted in aqueous mounting medium with anti-fading agents (Biomeda) and imaged on the Zeiss LSM 510 confocal laser scanning microscope. Optical cross-sections (X-Z images) of pupal wings in Figs. 2-4 were compiled from multiple X-Y images (1 μm thick) to form the 15-35 μm X-Z images shown. Fig. 6 shows representative 1 μm thick confocal images in the X-Y plane through the center of the dorsal and ventral cell layers of pupal wings. Images were processed using the LSM Imager Browser and Photoshop.

RNAi in Drosophila cell culture- For the generation of dsRNA, regions from each gene of interest (YFP, *mys*, *tiggrin* or *pgant3*) were amplified using primers containing T7 RNA polymerase binding sites and gene-specific sequences to produce ~500 bp fragments containing T7 promoters at the 5' ends. We selected regions for dsRNA generation by using the off-target sequence search tool on the *Drosophila* RNAi Screening Center (DRSC) website (http:// www.flyrnai.org/ RNAi_primer_design.html), in an effort to minimize any potential off-target effects. The off-target size was set as low as 16 nt for each analysis. Two regions for dsRNA generation were chosen for the *pgant3* gene and for the *tiggrin* gene to verify knockdown and cellular phenotypes observed. All primer sequences used for dsRNA generation are listed in Supplemental Table I.

PCR products from the above-mentioned primer pairs were purified and used as templates to produce RNA using the MEGASCRIPT T7 transcription kit (Ambion). RNA was LiCl precipitated, resuspended in water, incubated at 65ºC for 30 min and then slow-cooled to room temperature to allow annealing. dsRNA formed was then stored at -20 ºC.

Drosophila cells were grown in Schneider's medium (Invitrogen) with 10% heat- inactivated FBS (Invitrogen) at 25ºC in culture flasks. RNAi was performed as described on the DRSC website (http://flyrnai.org/ RNAi_FAQ_rnai_on_cc.html). Briefly, 2×10^5 S2R+ cells in 250μl serum-free media were added to each well of a 24-well plate. dsRNA (7μg) was added to each well and plates were mixed back and forth. The cells were then incubated for 30 min at room temperature before adding 750μl medium containing 10% heat-inactivated fetal bovine serum (Invitrogen).

Cells were grown for 4-6 days at 25 ºC. Each experiment was performed with two independent dsRNAs to *pgant3* to verify gene specific knockdown and observed phenotypes.

After dsRNA treatment, cells were fixed in 4% formaldehyde-phosphate-buffered saline (PBS) (Electron Microscopy Science) and then washed twice in PBS with 0.1% Triton X-100. Staining was then performed using TRITC-phalloidin (Sigma) and DAPI, followed by washes in PBS. Cells were examined using a Zeiss Axiophot microscope.

Cell adhesion assays- After incubating with dsRNA for 5 days, S2R+ cells were replated on glass slides and allowed to spread for 4 hours before fixing. S2 cells treated with dsRNA were replated on glass slides coated with 0.5mg/ml concanavalin A (Con A) and allowed to spread for 2 hours (42). After fixing, cells were stained with TRITC-phalloidin and DAPI.

Quantitative cell adhesion assays were performed on S2R+ cells after incubation with dsRNA. S2R+ cells were harvested and resuspended in the medium at a density of 2×10^5 cells/ml. 100 μl cell suspension was seeded into each well and then incubated for an additional 2hr at 25ºC. After removing the non-adherent cells, 150 μl 0.2% crystal violet (Sigma) aqueous solution in 20% methanol was added to stain the cells that remained attached. Wells were washed with Milli-Q water twice and then air-dried. Finally, cells were dissolved in 150 μl 1% SDS. The optical density at 570nm was measured using a Microplate Reader (TECAN). Cells adhesion assays were performed in triplicate and in multiple independent experiments. The data shown in Fig. 7C is representative of one experiment performed in triplicate.

Western blotting- Protein extracts were prepared from staged pupal wing discs of wild type and $pgant3^{m1}/pgant3^{m2}$ mutants as described (43). Samples were electrophoresed under reducing conditions in a 4-12% SDS-PAGE gradient gel and transferred to nitrocellulose membranes. Membranes were blocked with 1x blocking buffer (Sigma) and then incubated with an antibody to tiggrin (dilution, 1:500) or the Tn antibody (dilution, 1:500) and developed with HRP-conjugated mouse IgG (dilution, 1:2000) (Cell Signaling Technology) or HRP-conjugated mouse IgM (dilution, 1:10,000) (Stressgen Bioreagents) secondary antibodies, respectively. The upper band detected by the tiggrin antibody is not specific to tiggrin, as it is still present in tig^x homozygous mutants.

Quantitive real-time PCR- Cells were lysed and RNA was extracted using the RNAqueous-4 PCR kit (Ambion). cDNA synthesis was performed using the iScript cDNA synthesis kit (Bio-Rad). Quantitative real-time PCR (QPCR) primers for each *pgant* gene were described previously (20). QPCR was performed on a MyiQ real time PCR thermocycler (Bio-Rad) using the SYBR-Green PCR Master Mix (Bio-Rad). Analyzed products were assayed in triplicate and in multiple independent experiments.

RESULTS

Point mutations that disrupt pgant3 catalytic activity result in wing blistering and abrogation of tiggrin glycosylation. Previous work from our group demonstrated that a transposon insertion mutation in *pgant3*, which encodes an enzyme responsible for the initiation of mucin-type O-glycosylation, resulted in abrogation of *pgant3* expression and subsequent disruption of cell adhesion in the adult wing (20). We set out to further examine the role of O-glycosylation in wing blade adhesion by generating additional *pgant3* mutations that specifically affect catalytic activity. Through EMS mutagenesis, we obtained two novel point mutations in the coding region of *pgant3* (Fig. 1A). One mutation, $pgant3^{m1}$, is a C to T transition that changes a conserved arginine to a cysteine at

amino acid position 130. *pgant3*^{m1}, like wild type *pgant3*, encodes a protein that is localized properly to the Golgi apparatus and is stably expressed in cell culture (Fig. 1B and C). However, the PGANT3^{m1} protein fails to glycosylate substrates in in vitro glycosyltransferase reactions, indicating that this mutation specifically compromises enzymatic activity (Fig. 1D). The second mutation, *pgant3*^{m2}, is a G to A transition that creates a stop codon at amino acid 609, deleting the C-terminal 59 amino acids of the enzyme. This truncation results in an unstable protein that is not properly localized to the Golgi apparatus (Fig.1B). Additionally, we were not able to stably express the *pgant3*^{m2} mutant as a secreted, recombinant protein to perform in vitro enzymatic assays (Fig. 1C).

Flies carrying the original transposon mutation (*pgant3*^{c01318}), the *pgant3*^{m1} mutation or *pgant3*^{m2} mutation were crossed to assess the effect of the new *pgant3* point mutations on wing blistering frequency in adults (Table I and Fig. 1E). While heterozygous mutants displayed no effect on wing integrity, all transheterozygous mutants (*pgant3*^{m1}/*pgant3*^{m2}, *pgant3*^{m1}/*pgant3*^{c01318}, or *pgant3*^{m2}/*pgant3*^{c01318}) as well as mutants over a deficiency for the region (*pgant3*^{m1}/*Df(2R)Exel6283*, *pgant3*^{m2}/*Df(2R)Exel6283*, or *pgant3*^{c01318}/*Df(2R)Exel6283*) showed a high frequency of wing blistering (Table I). Additionally, these point mutants also displayed a loss of tiggrin glycosylation (Fig. 1F and G), as was seen previously for the transposon mutant (20). Because the *pgant3*^{m1} mutation (which forms a stable protein yet is catalytically inactive) resulted in wing blistering when combined with other *pgant3* mutations, we conclude that the loss of PGANT3 glycosyltransferase activity (and not simply loss of the PGANT3 protein) is responsible for the loss of wing integrity. This indicates that PGANT3 function in the developing wing is dependent upon its glycosyltransferase activity, and not on a glycosylation-independent chaperone function seen previously for other glycosyltransferases (44,45).

pgant3 genetically interacts with if (αPS2 integrin) to modulate cell adhesion. Prior studies from our group showed a genetic interaction between *pgant3* and *tiggrin* (20), demonstrating a functional consequence of PGANT3 activity on tiggrin-mediated cell adhesion. We next investigated whether a genetic interaction exists between *pgant3* mutants and an αPS2 integrin mutant (*if*^{3}). *if*^{3} mutants are hypomorphic and show a low level of wing blistering in a wild type background (9). Flies hemizygous for *if*^{3} in combination with the chromosome 2 used for mutagenesis (*if*^{3}/Y; +/+) displayed 17% wing blistering (Table II). As mentioned above, flies heterozygous for *pgant3*^{m1} or *pgant3*^{m2} displayed no wing blistering. However, flies that are both hemizygous for *if*^{3} and heterozygous for *pgant3*^{m1} (*if*^{3}/Y; *pgant3*^{m1}/+) or *pgant3*^{m2} (*if*^{3}/Y; *pgant3*^{m2}/+) displayed a dramatic increase in wing blistering (76% and 52%, respectively). Thus, mutations in *pgant3* and αPS2 integrin interact genetically to exacerbate the same morphological phenotype, demonstrating that *pgant3* modulates integrin-mediated cell adhesion in the developing wing.

Tiggrin and O-glycans are specifically localized during pupal wing development. Pupal wing development undergoes a series of apposition, adhesion, expansion and separation phases to ensure proper morphogenesis and establishment of cell contacts (46). To obtain insight into the role of O-glycans and tiggrin in integrin-mediated cell adhesion in the wing, we examined pupal wings at multiple different developmental stages. Both tiggrin and O-glycans were present in the developing wing and displayed dynamic localization throughout pupal wing development. Very specific localization of both was observed at the basal cell layer interface during two separate stages of

adhesion (6-8 hr after puparium formation (APF) and 34-42hr APF) (Fig. 2A-A' and D-E'), similar to what was previously seen for integrins (40,46). Localization of both O-glycans and tiggrin was diffuse during stages of separation of the epithelial cell layers (18-20 hr APF) (Fig. 2B and B'). Restoration of basal surface localization of both O-glycans and tiggrin begins to occur again as the second apposition phase takes place (24-26 hr APF) (Fig. 2C-C'). Thus, the specific localization of tiggrin and O-glycans to the basal region (where integrin is localized) during stages of cell adhesion further supports their involvement in integrin-mediated cell adhesion.

pgant3 mutant pupal wing discs show altered glycosylation and tiggrin localization. To investigate the specific role of *pgant3* in wing blade adhesion, we compared wild type and *pgant3* mutant wings at the adhesive stages of pupal wing development. Pupal wings at either 6-8 hrs APF or 34-36 hrs APF were stained for tiggrin, O-glycans and βPS integrin (Fig. 3). Optical X-Z cross-sections of the wings are shown. In wild type (WT) wings, tiggrin, O-glycans and βPS integrin all localize as a diffuse line across the center of the wing where the two cell layers begin to appose at 6-8 hr APF (Fig. 3A and C). This localization becomes much more distinct at 34-36 hr APF, when they are tightly localized at the basal surface of the dorsal/ventral cell layers (Fig. 3B and D). However, $pgant3^{m1}/pgant3^{m2}$ mutants displayed a reduction in O-glycosylation and a loss of tiggrin along the cell layer interface at both stages of wing development (Fig. 3), suggesting that either tiggrin stability or localization is altered in these mutants. The same altered tiggrin localization was also seen in $pgant3^{c01318}/pgant3^{c01318}$ transposon insertion mutants (Fig. 3A and B). O-glycosylation and tiggrin localization were restored upon excision of the transposon (Fig. 3A and B). Interestingly, βPS integrin was still present along the cell layer interface in *pgant3* mutants, indicating that the presence of tiggrin at this interface is not required for proper integrin localization and that the presence of βPS integrin is not sufficient to ensure tiggrin localization (Fig. 3C and D). However, βPS integrin staining was slightly more diffuse in the *pgant3* mutants, suggesting that disruption of tiggrin localization may influence integrin distribution.

To address whether other proteins are also mislocalized in *pgant3* mutants, we examined the localization of Fasciclin III and DE-cadherin (Fig. 4). High magnification images of pupal wings at stage 36 hr APF reveal that tiggrin staining is still seen within the cells of the $pgant3^{m1}/pgant3^{m2}$ and $pgant3^{m1}/$ *Df (2R)Exel6283* mutants (Fig. 4B-C''), but it is not precisely localized to the basal cell layer interface as in wild type pupal wings (Fig. 4A-A''). However, Fasciclin III and DE-cadherin, two membrane proteins with distinct localizations, showed no difference in staining patterns between wild type and *pgant3* mutant wings (Fig. 4D-I''). These results suggest that the loss of O-glycosylation specifically disrupts tiggrin localization.

pgant3 influences tiggrin secretion, not stability. The loss of tiggrin from the basal cell adhesive region could be due to altered tiggrin secretion, altered tiggrin retention along this region or an increase in tiggrin degradation. To distinguish between these possibilities, we performed western blots using extracts from *pgant3* mutant and wild type pupal wings (Fig. 5). No significant difference in the amount or size of tiggrin was seen between mutant and wild type wings at multiple developmental stages (Fig.5A, B and C), suggesting that loss of tiggrin at the cell layer interface in *pgant3* mutant wings is not due to degradation.

To examine the affect of O-glycosylation on tiggrin secretion, we stained wild type and *pgant3* mutant pupal wings for tiggrin and DE-cadherin (to outline the cells). Multiple

confocal X-Y cross sections (1 μm) through the center of both the dorsal and ventral cell layers were taken to visualize whether tiggrin is present at the cell boundaries defined by DE-cadherin staining. Confocal images revealed that while tiggrin is present along the outer membrane of cells in wild type wings, it is largely absent from this region in *pgant3* mutant wing cells (Fig. 6). Additionally, tiggrin staining in *pgant3* mutant wings is primarily seen in punctate structures inside the cell borders, indicating an accumulation of tiggrin within the cells of *pgant3* mutant wings. These results strongly support a role for O-glycosylation in proper tiggrin secretion.

RNAi to pgant3 affects integrin-mediated cell adhesion in cell culture. To further investigate the role of *pgant3* in cell adhesion, we employed a *Drosophila* cell line that has been used to examine integrin-mediated cell adhesion (11,42). S2R+ cells, an adherent line of embryonic origin, were treated with a non-specific dsRNA (YFP), dsRNA to a βPS integrin known to cause cell adhesion defects (*mys*) (47), dsRNA to *tiggrin* or dsRNA to *pgant3*. Treated cells were fixed and stained with phalloidin to detect changes in cell spreading, shape and adhesion. Untreated cells or cells treated with YFP dsRNA had highly developed actin-based lamellae and were well-spread on cell culture dishes. As seen previously, cells treated with *mys* dsRNA became round and non-adherent, with a dramatic actin fibril reorganization (Fig. 7A and C). Additionally, cells treated with dsRNA to *tiggrin* were also less adherent (Fig. 7A and C). Interestingly, cells treated with *pgant3* dsRNA displayed a similar non-adherent phenotype, with treated cells becoming round, detaching from the dish, and displaying altered actin organization (Fig. 7A and C). The effects seen were verified with a second independent dsRNA to *pgant3* (data not shown) and the degree and specificity of *pgant3* knockdown was assessed by real time quantitative PCR (Fig. 7D). Additionally, we found that these morphological and cell adhesive changes were unique to *pgant3*, as RNAi to the other members of the *pgant* family did not result in similar changes (data not shown). Thus, as is the case in vivo, *pgant3* appears to be required for proper integrin-mediated cell adhesion of S2R+ cells in culture.

To address the specificity of *pgant3* in integrin-mediated cell adhesion, we compared the effects of *pgant3* knockdown in a *Drosophila* cell line that utilizes different adhesion mechanisms. S2 cells, which are normally non-adherent, will adhere to concanavalin A (Con A) coated surfaces via an integrin-independent mechanism (42), in contrast to the integrin-dependent adherence of S2R+ cells. When βPS integrin (*mys*) or *tiggrin* gene expression in S2 cells were reduced by RNAi, S2 cells remained attached to the Con A coated surface, with no noticeable changes in cell morphology or spreading (42) (Fig. 7B). Similarly, RNAi to *pgant3* in S2 cells significantly reduced *pgant3* gene expression but had no effect on cell adhesion (Fig. 7B and E). These data suggest that the cell adhesion defects caused by RNAi to *pgant3* are unique to S2R+ cells and lend further support for a model where *pgant3* is involved specifically in integrin-mediated cell adhesion. Taken together, our data support a model where *pgant3* affects integrin-mediated cell adhesion in the developing wing by influencing the secretion of the integrin-ligand, tiggrin.

DISCUSSION

In this study, we demonstrate that O-glycosylation influences the secretion and localization of a specific matrix protein, altering the microenvironment of the wing and resulting in direct biological consequences during development. Tiggrin, an secreted ECM protein known to bind integrin and mediate cell

adhesion (3,18), is normally O-glycosylated and located at the adhesive interface between the two epithelial cell layers of the developing wing. This area of the developing wing, where integrins are also localized, governs cell-cell contacts and proper wing blade formation. In *pgant3* mutants, tiggrin is not O-glycosylated and fails to be secreted to this cell layer interface, resulting in cell adhesion defects. Disruption of tiggrin localization and cell adhesion are directly associated with the glycosylation status of tiggrin, as restoration of *pgant3* activity restores tiggrin glycosylation, localization, and wing integrity. Additionally, a *pgant3* mutant that is stably expressed, but lacks catalytic activity, demonstrates that these effects are due to the glycosyltransferase activity of PGANT3 and not due to a chaperone function in the absence of enzymatic activity. This distinguishes the effects of PGANT3 from those of another glycosyltransferase (O-fucosyltransferase 1) that influences Notch transport by functioning as a chaperone in the absence of glycosyltransferase activity (44,45). Altogether, our studies provide the first evidence for the role of mucin-type O-glycans in proper secretion and localization of extracellular matrix proteins during eukaryotic development.

Our data further demonstrate that the influence of O-glycosylation on tiggrin localization to the basal matrix is due to effects on tiggrin secretion. While other studies suggest that mucin-type O-glycans may influence protein stability, as is thought to be the case for FGF23 in familial tumoral calcinosis (26,31,32), we do not see evidence of altered tiggrin stability in pupal wings. Rather, our analysis of tiggrin localization in *pgant3* mutant wings cells revealed dramatic intracellular accumulation, indicating defects in tiggrin secretion. Prior studies examining proteins known to be glycosylated have suggested roles for O-glycans in secretion. For example, regions that are crucial for secretion or apical sorting of certain proteins have been shown to be rich in O-glycosylated residues (36,48). Additionally, Muc4, a highly O-glycosylated protein, influences ErbB2 and ErbB3 receptor trafficking to the cell surface in cultured cells (49). Cell culture studies using competitive inhibitors of O-glycan extension resulted in reduced trafficking of certain proteins (33-36); however, these inhibitors also influence other forms of glycosylation. Studies examining protein distribution in subregions of the Golgi complex in larval imaginal discs, found that those containing O-linked GalNAc were present predominantly in basally-located Golgi units, suggesting that this polarized distribution may influence apicobasal polarity in these tissues (50). Here, we provide direct evidence for the role of mucin-type O-glycans in modulating proper secretion to this basal region in vivo by examining a specific substrate in a glycosyltransferase mutant background. Given that the multiple *pgant* genes responsible for initiating mucin-type O-glycosylation (22,39) have unique tissue and stage-specific patterns of expression (23,51-53), it is likely that specific *pgant* family members may be playing unique roles in the secretion and localization of proteins within diverse cell types.

Our study further provides the first demonstration of a specific role for O-glycosylation in integrin-mediated cell adhesion events by demonstrating a genetic interaction between αPS2 integrin and *pgant3*. Mutations in *pgant3* genetically interact with αPS2 integrin mutants to increase wing blistering, providing a functional connection between O-glycosylation and cell adhesion mediated by integrins. Additionally, *Drosophila* cell culture assays demonstrated that RNAi to *pgant3* disrupted integrin–dependent cell adhesion, but did not affect integrin-independent cell adhesion. Altogether, our studies demonstrate a specific role for O-glycosylation in integrin-mediated cell

adhesion that is dictated by the influence of O-glycans on integrin-ligand secretion and localization. These results have implications for this protein modification in other developmental and pathological processes involving integrins.

pgant3 mutations did not appear to alter the localization of other proteins present in the developing wing. The specific localization of the cell membrane proteins, DE-cadherin and Fasciclin III were unchanged in *pgant3* mutants, suggesting that loss of O-glycosylation in this context is not leading to global changes in cell polarity as was seen previously for mutations in *pgant35A*, which disrupted tracheal cell polarity and diffusion barrier formation (28). The specific effect of *pgant3* on cell adhesion is supported by the fact that adult wings in *pgant3* mutants are, with the exception of blisters, normal in morphology. Additionally, β-integrin was still found at the cell layer interface, albeit in a more diffuse pattern, again indicating that *pgant3* mutations do not result in an overall disruption of the basal surface. These data indicate that PGANT3 modulates cell adhesive functions by influencing the secretion of a specific ECM component. It will be interesting to see if other ECM components are influenced by PGANT3 or other PGANT family members in the future.

This study has implications for the role of O-glycosylation in other developing systems and in certain diseases (22). For example, our data could provide insight into the long-standing correlation between aberrant O-glycosylation and the progression of certain types of cancer (54-58). Indeed, recent work has demonstrated that germ-line and somatic mutations in a member of this glycosyltransferase family (GALNT12) are associated with colon cancer in humans (59). Additionally, deletion of an extending glycosyltransferase in mice results in increased susceptibility to colorectal tumors (60). While the molecular mechanisms underlying these associations are not known, our work supports a model where mutations in a glycosyltransferase could alter the composition of the secreted ECM or "microenvironment" surrounding cells, thus influencing adhesive, protective or signaling properties. Such an alteration in the microenvironment may influence the dialogue occurring between a cell and its surrounding matrix, thereby altering the susceptibility of cells/tissues to other genetic or environmental changes. Indeed, recent studies are focusing on the role of "tumor microenvironment" and the interplay between intra- and extracellular factors in cancer progression and metastasis (61). We have thus identified a factor that is capable of modifying a cell's microenvironment, resulting in direct consequences on cell adhesion. We are currently investigating whether other PGANT family members are capable of modulating secretion and ECM composition, and what role this may play in both development and disease.

References

1. Brower, D. L., Bunch, T. A., Mukai, L., Adamson, T. E., Wehrli, M., Lam, S., Friedlander, E., Roote, C. E., and Zusman, S. (1995) *Development* **121**(5), 1311-1320
2. Bloor, J. W., and Brown, N. H. (1998) *Genetics* **148**(3), 1127-1142
3. Bunch, T. A., Graner, M. W., Fessler, L. I., Fessler, J. H., Schneider, K. D., Kerschen, A., Choy, L. P., Burgess, B. W., and Brower, D. L. (1998) *Development* **125**(9), 1679-1689
4. Prokop, A., Martin-Bermudo, M. D., Bate, M., and Brown, N. H. (1998) *Dev Biol* **196**(1), 58-76

5. Walsh, E. P., and Brown, N. H. (1998) *Genetics* **150**(2), 791-805
6. Araujo, H., Negreiros, E., and Bier, E. (2003) *Development* **130**(16), 3851-3864
7. Brower, D. L. (2003) *Curr Opin Cell Biol* **15**(5), 607-613
8. Narasimha, M., and Brown, N. H. (2004) *Curr Biol* **14**(5), 381-385
9. Brabant, M. C., and Brower, D. L. (1993) *Dev Biol* **157**(1), 49-59
10. Prout, M., Damania, Z., Soong, J., Fristrom, D., and Fristrom, J. W. (1997) *Genetics* **146**(1), 275-285
11. Brown, N. H., Gregory, S. L., Rickoll, W. L., Fessler, L. I., Prout, M., White, R. A., and Fristrom, J. W. (2002) *Dev Cell* **3**(4), 569-579
12. Dominguez-Gimenez, P., Brown, N. H., and Martin-Bermudo, M. D. (2007) *J Cell Sci* **120**(Pt 6), 1061-1071
13. Chanana, B., Graf, R., Koledachkina, T., Pflanz, R., and Vorbruggen, G. (2007) *Mech Dev* **124**(6), 463-475
14. Subramanian, A., Wayburn, B., Bunch, T., and Volk, T. (2007) *Development* **134**(7), 1269-1278
15. Schock, F., and Perrimon, N. (2003) *Genes Dev* **17**(5), 597-602
16. Bokel, C., and Brown, N. H. (2002) *Dev Cell* **3**(3), 311-321
17. Devenport, D., Bunch, T. A., Bloor, J. W., Brower, D. L., and Brown, N. H. (2007) *Dev Biol* **308**(2), 294-308
18. Fogerty, F. J., Fessler, L. I., Bunch, T. A., Yaron, Y., Parker, C. G., Nelson, R. E., Brower, D. L., Gullberg, D., and Fessler, J. H. (1994) *Development* **120**(7), 1747-1758
19. Graner, M. W., Bunch, T. A., Baumgartner, S., Kerschen, A., and Brower, D. L. (1998) *J Biol Chem* **273**(29), 18235-18241
20. Zhang, L., Zhang, Y., and Hagen, K. G. (2008) *J Biol Chem* **283**(49), 34076-34086
21. Ten Hagen, K. G., Fritz, T. A., and Tabak, L. A. (2003) *Glycobiology* **13**(1), 1R-16R
22. Tian, E., and Ten Hagen, K. G. (2009) *Glycoconj J* **26**(3), 325-334
23. Ten Hagen, K. G., Zhang, L., Tian, E., and Zhang, Y. (2009) *Glycobiology* **19**(2), 102-111
24. Ten Hagen, K. G., and Tran, D. T. (2002) *J Biol Chem* **277**(25), 22616-22622
25. Xia, L., Ju, T., Westmuckett, A., An, G., Ivanciu, L., McDaniel, J. M., Lupu, F., Cummings, R. D., and McEver, R. P. (2004) *J Cell Biol* **164**(3), 451-459
26. Topaz, O., Shurman, D. L., Bergman, R., Indelman, M., Ratajczak, P., Mizrachi, M., Khamaysi, Z., Behar, D., Petronius, D., Friedman, V., Zelikovic, I., Raimer, S., Metzker, A., Richard, G., and Sprecher, E. (2004) *Nat Genet* **36**(6), 579-581
27. Ju, T., and Cummings, R. D. (2005) *Nature* **437**(7063), 1252
28. Tian, E., and Ten Hagen, K. G. (2007) *J Biol Chem* **282**(1), 606-614
29. Tenno, M., Ohtsubo, K., Hagen, F. K., Ditto, D., Zarbock, A., Schaerli, P., von Andrian, U. H., Ley, K., Le, D., Tabak, L. A., and Marth, J. D. (2007) *Mol Cell Biol* **27**(24), 8783-8796
30. Fu, J., Gerhardt, H., McDaniel, J. M., Xia, B., Liu, X., Ivanciu, L., Ny, A., Hermans, K., Silasi-Mansat, R., McGee, S., Nye, E., Ju, T., Ramirez, M. I., Carmeliet, P., Cummings, R. D., Lupu, F., and Xia, L. (2008) *J Clin Invest* **118**(11), 3725-3737
31. Ichikawa, S., Guigonis, V., Imel, E. A., Courouble, M., Heissat, S., Henley, J. D., Sorenson, A. H., Petit, B., Lienhardt, A., and Econs, M. J. (2007) *J Clin Endocrinol Metab* **92**(5), 1943-1947
32. Frishberg, Y., Ito, N., Rinat, C., Yamazaki, Y., Feinstein, S., Urakawa, I., Navon-Elkan, P., Becker-Cohen, R., Yamashita, T., Araya, K., Igarashi, T., Fujita, T., and Fukumoto, S. (2007) *J Bone Miner Res* **22**(2), 235-242

33. Delannoy, P., Kim, I., Emery, N., De Bolos, C., Verbert, A., Degand, P., and Huet, G. (1996) *Glycoconj J* **13**(5), 717-726
34. Huet, G., Hennebicq-Reig, S., de Bolos, C., Ulloa, F., Lesuffleur, T., Barbat, A., Carriere, V., Kim, I., Real, F. X., Delannoy, P., and Zweibaum, A. (1998) *J Cell Biol* **141**(6), 1311-1322
35. Gouyer, V., Leteurtre, E., Delmotte, P., Steelant, W. F., Krzewinski-Recchi, M. A., Zanetta, J. P., Lesuffleur, T., Trugnan, G., Delannoy, P., and Huet, G. (2001) *J Cell Sci* **114**(Pt 8), 1455-1471
36. Potter, B. A., Hughey, R. P., and Weisz, O. A. (2006) *Am J Physiol Cell Physiol* **290**(1), C1-C10
37. Thibault, S. T., Singer, M. A., Miyazaki, W. Y., Milash, B., Dompe, N. A., Singh, C. M., Buchholz, R., Demsky, M., Fawcett, R., Francis-Lang, H. L., Ryner, L., Cheung, L. M., Chong, A., Erickson, C., Fisher, W. W., Greer, K., Hartouni, S. R., Howie, E., Jakkula, L., Joo, D., Killpack, K., Laufer, A., Mazzotta, J., Smith, R. D., Stevens, L. M., Stuber, C., Tan, L. R., Ventura, R., Woo, A., Zakrajsek, I., Zhao, L., Chen, F., Swimmer, C., Kopczynski, C., Duyk, G., Winberg, M. L., and Margolis, J. (2004) *Nat Genet* **36**(3), 283-287
38. Lewis, E.B. and Bacher, F. (1968). *Drosophila Information Service* **43**,193.8
39. Ten Hagen, K. G., Tran, D. T., Gerken, T. A., Stein, D. S., and Zhang, Z. (2003) *J Biol Chem* **278**(37), 35039-35048
40. O'Keefe, D. D., Prober, D. A., Moyle, P. S., Rickoll, W. L., and Edgar, B. A. (2007) *Dev Biol* **311**(1), 25-39
41. Avichezer, D., Springer, G. F., Schechter, B., and Arnon, R. (1997) *Int J Cancer* **72**(1), 119-127
42. Jani, K., and Schock, F. (2007) *J Cell Biol* **179**(7), 1583-1597
43. Pickup, A. T., and Banerjee, U. (1999) *Dev Biol* **205**(2), 254-259
44. Okajima, T., Xu, A., Lei, L., and Irvine, K. D. (2005) *Science* **307**(5715), 1599-1603
45. Okajima, T., Reddy, B., Matsuda, T., and Irvine, K. D. (2008) *BMC Biol* **6,**1
46. Fristrom, D., Wilcox, M., and Fristrom, J. (1993) *Development* **117**(2), 509-523
47. Kiger, A. A., Baum, B., Jones, S., Jones, M. R., Coulson, A., Echeverri, C., and Perrimon, N. (2003) *J Biol* **2**(4), 27
48. Yeaman, C., Le Gall, A. H., Baldwin, A. N., Monlauzeur, L., Le Bivic, A., and Rodriguez-Boulan, E. (1997) *J Cell Biol* **139**(4), 929-940
49. Funes, M., Miller, J. K., Lai, C., Carraway, K. L., 3rd, and Sweeney, C. (2006) *J Biol Chem* **281**(28), 19310-19319
50. Yano, H., Yamamoto-Hino, M., Abe, M., Kuwahara, R., Haraguchi, S., Kusaka, I., Awano, W., Kinoshita-Toyoda, A., Toyoda, H., and Goto, S. (2005) *Proc Natl Acad Sci U S A* **102**(38), 13467-13472
51. Kingsley, P. D., Hagen, K. G., Maltby, K. M., Zara, J., and Tabak, L. A. (2000) *Glycobiology* **10**(12), 1317-1323
52. Tian, E., and Ten Hagen, K. G. (2006) *Glycobiology* **16**(2), 83-95
53. Tian, E., and Ten Hagen, K. G. (2007) *Glycobiology* **17**(8), 820-827
54. Kim, Y. S., Gum, J., Jr., and Brockhausen, I. (1996) *Glycoconj J* **13**(5), 693-707
55. Kim, Y. J., and Varki, A. (1997) *Glycoconj J* **14**(5), 569-576
56. Springer, G. F. (1997) *J Mol Med* **75**(8), 594-602
57. Ono, M., and Hakomori, S. (2004) *Glycoconj J* **20**(1), 71-78
58. Fuster, M. M., and Esko, J. D. (2005) *Nat Rev Cancer* **5**(7), 526-542
59. Guda, K., Moinova, H., He, J., Jamison, O., Ravi, L., Natale, L., Lutterbaugh, J., Lawrence, E., Lewis, S., Willson, J. K., Lowe, J. B., Wiesner, G. L., Parmigiani, G., Barnholtz-Sloan, J.,

Dawson, D. W., Velculescu, V. E., Kinzler, K. W., Papadopoulos, N., Vogelstein, B., Willis, J., Gerken, T. A., and Markowitz, S. D. (2009) *Proc Natl Acad Sci U S A* **106**(31), 12921-12925

60. An, G., Wei, B., Xia, B., McDaniel, J. M., Ju, T., Cummings, R. D., Braun, J., and Xia, L. (2007) *J Exp Med* **204**(6), 1417-1429
61. Xu, R., Boudreau, A., and Bissell, M. J. (2009) *Cancer Metastasis Rev* **28**(1-2), 167-176

FOOTNOTES

We would like to sincerely thank our colleagues for many helpful discussions. We thank Drs. R. Cummings and T. Ju for the kind gift of the Tn antibody; and Drs. J. Fessler and L. Fessler for the kind gift of the tiggrin antibody. We thank Dr. J. Kennison for the kind gift of fly stocks. Finally, we also thank the Bloomington Stock Center and the Developmental Studies Hybridoma Bank for providing fly stocks, antibodies and other reagents. This research was supported by the Intramural Research Program of the NIDCR at the National Institutes of Health.

The abbreviations used are: ppGalNAcT or PGANT or *pgant*, UDP GalNAc:polypeptide N-acetylgalactosaminyltransferase;; GalNAc, N-acetylgalactosamine; ECM, extracellular matrix; qPCR, quantitative polymerase chain reaction; RNAi, RNA interference; YFP, yellow fluorescence protein; dsRNA, double stranded RNA.

FIGURE LEGENDS

Fig. 1. *pgant3* point mutations cause wing blistering and loss of tiggrin O-glycosylation. (A) Two point mutations in the coding region of *pgant3* were obtained by EMS mutagenesis. The *pgant3*^{m1} mutation changes a conserved arginine (R) to a cysteine (C) at amino acid 130. The *pgant3*^{m2} mutation changes a tryptophan (W) to a stop codon at amino acid 609 in the lectin-like region, deleting the C-terminal portion of the enzyme. (B) Expression of recombinant wild type *pgant3* (pIB-pgant3-V5), *pgant3*^{m1} (pIB-m1-V5) and *pgant3*^{m2} (pIB-m2-V5) in *Drosophila* S2R+ cells. Cells were then stained for V5 and the Golgi marker, GM130, revealing Golgi-localization of wild type *pgant3* and *pgant3*^{m1}. (C) Expression of secreted forms of *pgant3* in COS7 cells demonstrates that wild type *pgant3* and *pgant3*^{m1} are stably expressed as recombinant proteins while *pgant3*^{m2} is not. (D) The *pgant3*^{m1} mutation results in loss of glycosyltransferase activity. Equal relative amounts of wild type *pgant3* (WT, *circles*) and *pgant3*^{m1} (m1, *squares*) proteins (as determined by western blotting) produced and purified from COS7 cells were used with increasing concentrations of acceptor substrate (EA2) in enzyme assays as described in Experimental Procedures. All assays were performed in triplicate. Error bars indicate standard deviation. (E) Homozygous *pgant3* mutants (*pgant3*^{m1}/*pgant3*^{m2}) have wing blisters, indicative of cell adhesion defects. Western blots of proteins from wing discs of wild type (WT), the parental line used for mutagenesis (cn bw sp) and *pgant3*^{m1}/*pgant3*^{m2} mutants (m1/m2) probed with the Tn antibody (F) or an antibody to tiggrin (G) demonstrate that tiggrin is present but not O-glycosylated in *pgant3*^{m1}/*pgant3*^{m2} mutants. Protein size standards are shown to the right. Red arrowheads indicate the position of the glycosylated tiggrin band.

Fig. 2. Tiggrin and O-glycans show dynamic and specific localization during pupal wing development. Shown are stages of wild type pupal wing development 6-8 hrs after puparium formation (APF) (6-8hr APF), 18-20 hrs after puparium formation (18-20hr APF), 24-26 hrs after puparium formation (24-26hr APF), 34-36 hrs after puparium formation (34-36hr APF) and 40-42 hrs

after puparium formation (40-42hr APF). Wings were stained for tiggrin (green), O-glycans (red) and DAPI (blue). Merged images show tiggrin and O-glycan co-staining in yellow. Images shown are X-Y sections (A, B, C, D, E) or X-Z optical cross-sections (A', B', C', D', E'). White dashed lines indicate regions used to produce X-Z optical cross sections. Arrowheads at the right denote the basal dorsal/ventral cell layer interface and asterisks (*) denote the position of wing veins. Black bar = 100μm.

Fig. 3. Localization of tiggrin, βPS integrin and O-glycans in wild type and *pgant3* mutant pupal wings. Pupal wings from either wild type (WT), *pgant3*^{m1}/*pgant3*^{m2} homozygous point mutants (m1/m2), homozygous *pgant3*^{c01318}/*pgant3*^{c01318} transposon insertion mutation (Transposon) or the *pgant3*$^{hopout\#7}$/*pgant3*$^{hopout\#7}$ transposon excision line (Transposon excision) were stained for tiggrin (green) (A and B), βPS integrin (green) (C and D) and O-glycans (red) (A-D). Merged images show co-staining in yellow. X-Z optical cross-sections of confocal images of pupal wings at 6-8 hrs APF (A and C) or 34-36 hrs APF (B and D) are shown. Nuclei were detected with DAPI. Arrowheads at the right denote the basal dorsal/ventral cell layer interface and asterisks (*) denote the position of wing veins. Black bar = 100μm.

Fig. 4. Localization of tiggrin, but not other proteins, is affected in *pgant3* mutant pupal wings. Wild type (WT) (A-A'', D-D'', and G-G''), *pgant3*^{m1}/*pgant3*^{m2} (m1/m2) (B-B'', E-E'' and H-H'') and *pgant3*^{m1}/*Df(2R)Exel6283* (m1/Df(2R)) (C-C'', F-F'' and I-I'') pupal wings at 36 hrs APF were stained with tiggrin (green) (A-C''); Fasciclin III (red) (D-F''); and DE-cadherin (purple) (G-H''). Shown are X-Z optical cross-sections of pupal wings with (A-I) or without (A'-I') DAPI staining of nuclei. Images are oriented so that dorsal is at the top and ventral is at the bottom. Arrowheads at the left denote the basal dorsal/ventral cell layer interface. X-Y confocal images of the basal region comprising the dorsal and ventral boundary (A''-I'') are also shown. In wild type wings 36 hrs APF, tiggrin localizes to the dorsal/ventral cell layer interface, where cell adhesion occurs. Mutations in *pgant3* result in loss of tiggrin localization at this interface, while DE-cadherin and Fasciclin III localizations are unaffected.

Fig. 5. Western blots of pupal wing extracts reveal no change in amount of tiggrin present in *pgant3* mutant wings relative to wild type. Equivalent amounts of protein extracts from wild type (WT) and *pgant3*^{m1}/*pgant3*^{m2} homozygous point mutants (m1/m2) at 4 hr APF (A), 8 hr APF (B) and 48 hr APF (C) were western blotted and probed with a tiggrin antibody. No significant change in the amount or size of tiggrin was seen when comparing wild type and *pgant3* mutant wings at various times during wing development. Size markers are shown to the left of each blot.

Fig. 6. *pgant3* mutations result in intracellular tiggrin accumulation. Wild type (A) and *pgant3*^{m1}/*Df(2R)Exel6283* (B) pupal wings at 36 hrs APF were stained for tiggrin (Tig) (red) and DE-cadherin (DE-cad) (green). Merged images are shown in yellow. Shown are representative X-Y confocal images (1 μm thick) of pupal wings in the center of the dorsal cell layer (Dorsal) and in the center of the ventral cell layer (Ventral). *pgant3* mutants show loss of tiggrin along cell membranes and accumulation within the cells of the dorsal and ventral cell layers.

Fig. 7. RNAi to *pgant3* results in cell adhesion defects in cells that undergo integrin-mediated

cell adherence. S2R+ (A) and S2 (B) cells were either untreated or treated with the dsRNA to *pgant3*, *tiggrin*, *mys* (βPS integrin) or YFP and then stained with phalloidin (Actin) and DAPI (Nuclei) to visualize cell spreading and adhesion. Decreases in S2R+-specific cell adhesion upon RNAi to *pgant3*, *tiggrin* or *mys* were quantitated as described in Experimental Procedures (C). No cell adhesion alterations were seen in S2 cells plated on Con A coated surfaces following treatment with dsRNA to *pgant3*, *tiggrin* or *mys* (B). Real time PCR analysis of the expression of all *pgant* family members in S2R+ cells (D) or S2 cells (E) confirmed that RNAi to *pgant3* resulted in a specific reduction in *pgant3* expression. RNA levels were normalized to 18S rRNA. Scale bars shown below panels (A) and (B) =20 μm. *, $p<0.05$; **, $p<0.01$. Error bars=standard deviation.

Table I. Frequency of wing blistering observed in *pgant3* mutants

Table II. Genetic interaction between *pgant3* and *if* (αPS2 integrin)

Supplemental Table I. Primer sequences for dsRNA generation

Fig.1

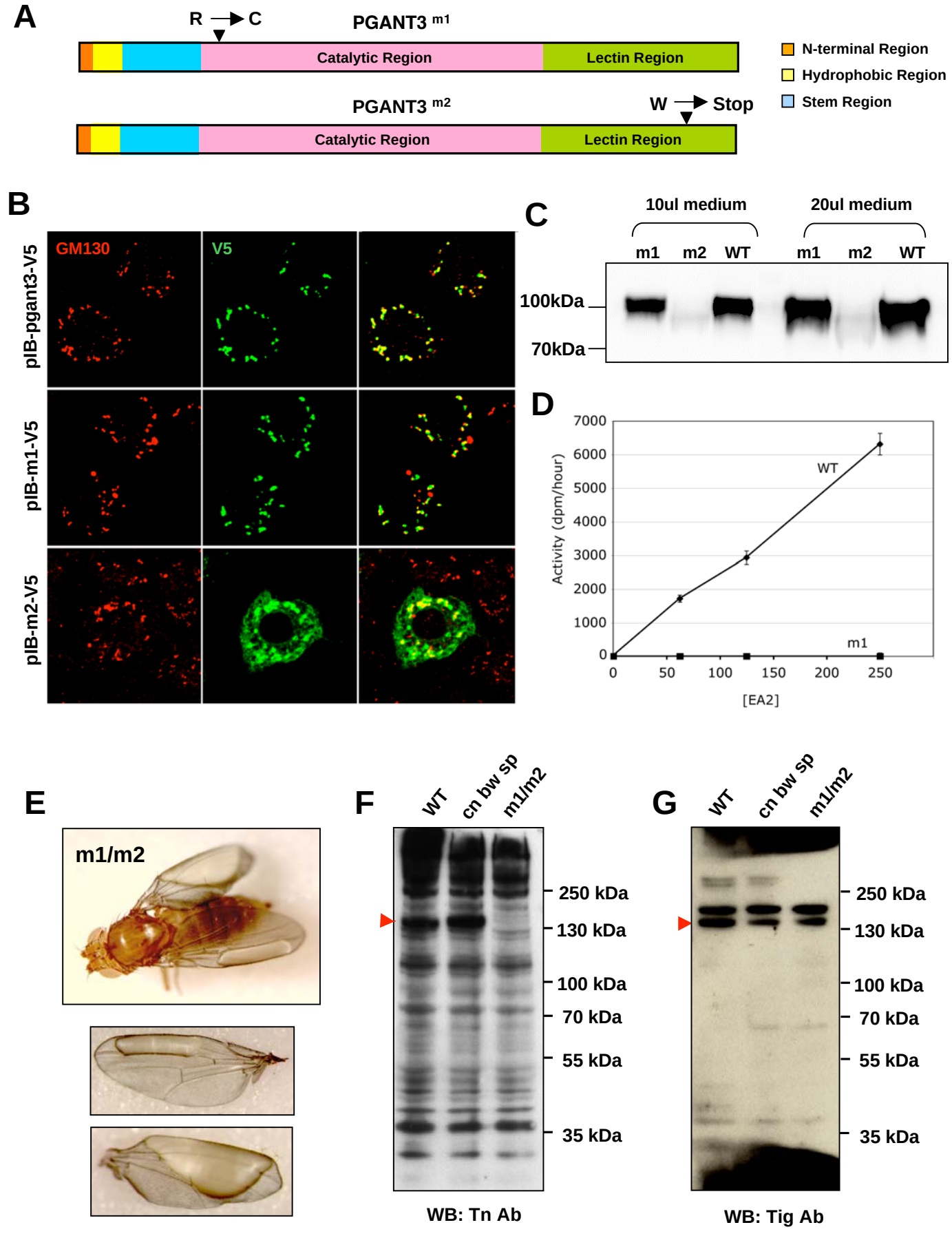

Fig.2

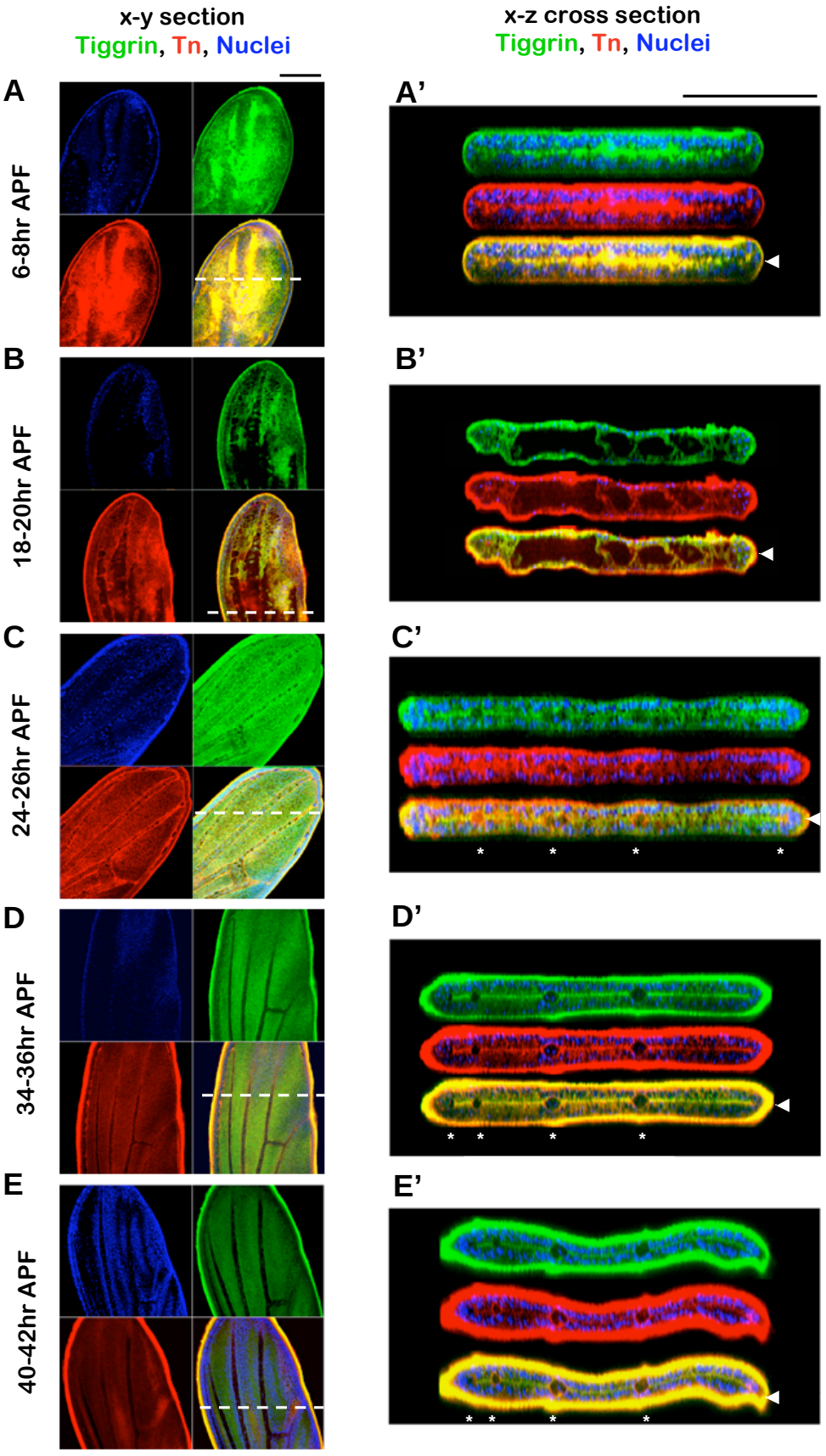

Fig. 3

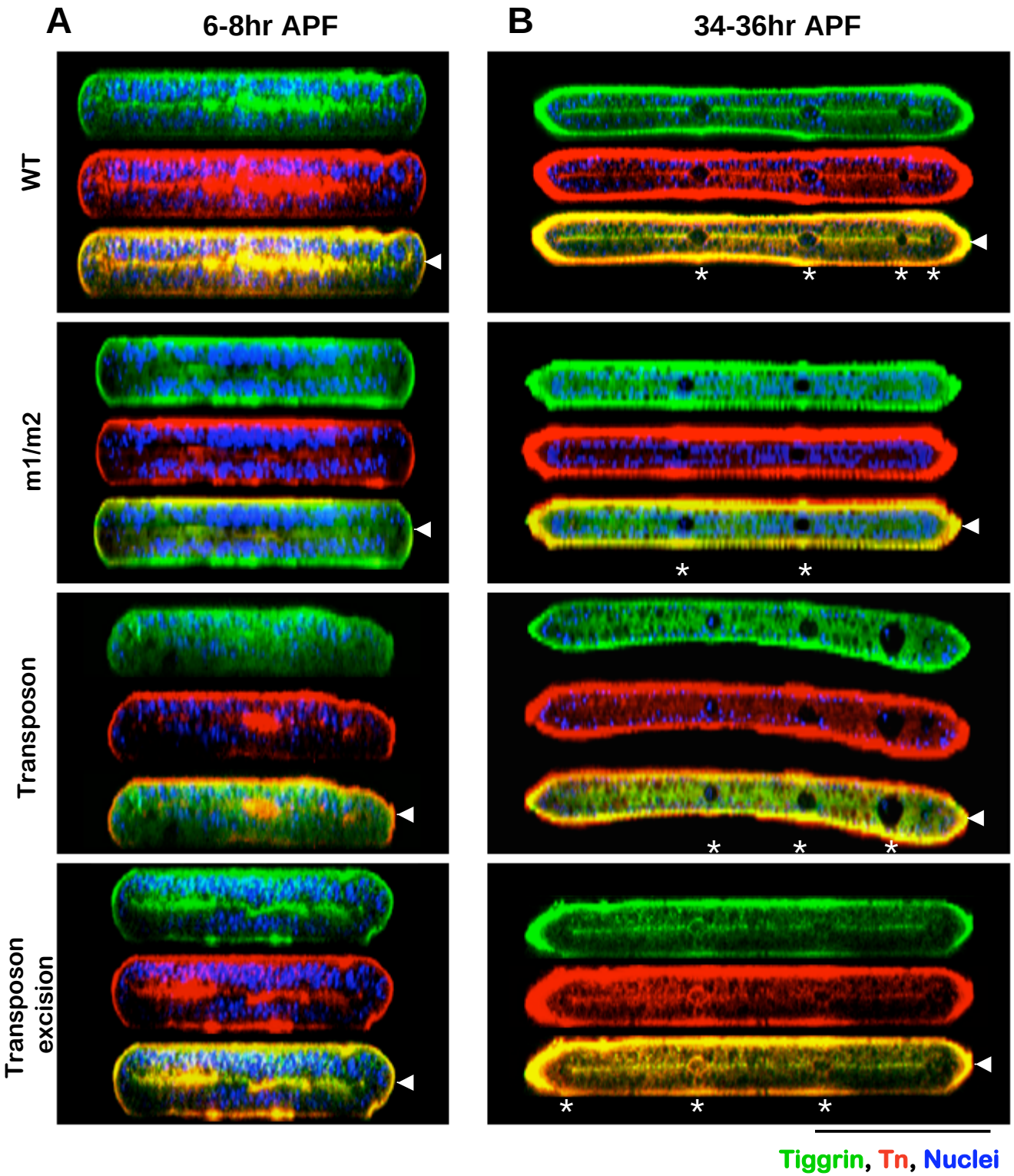

Fig. 3

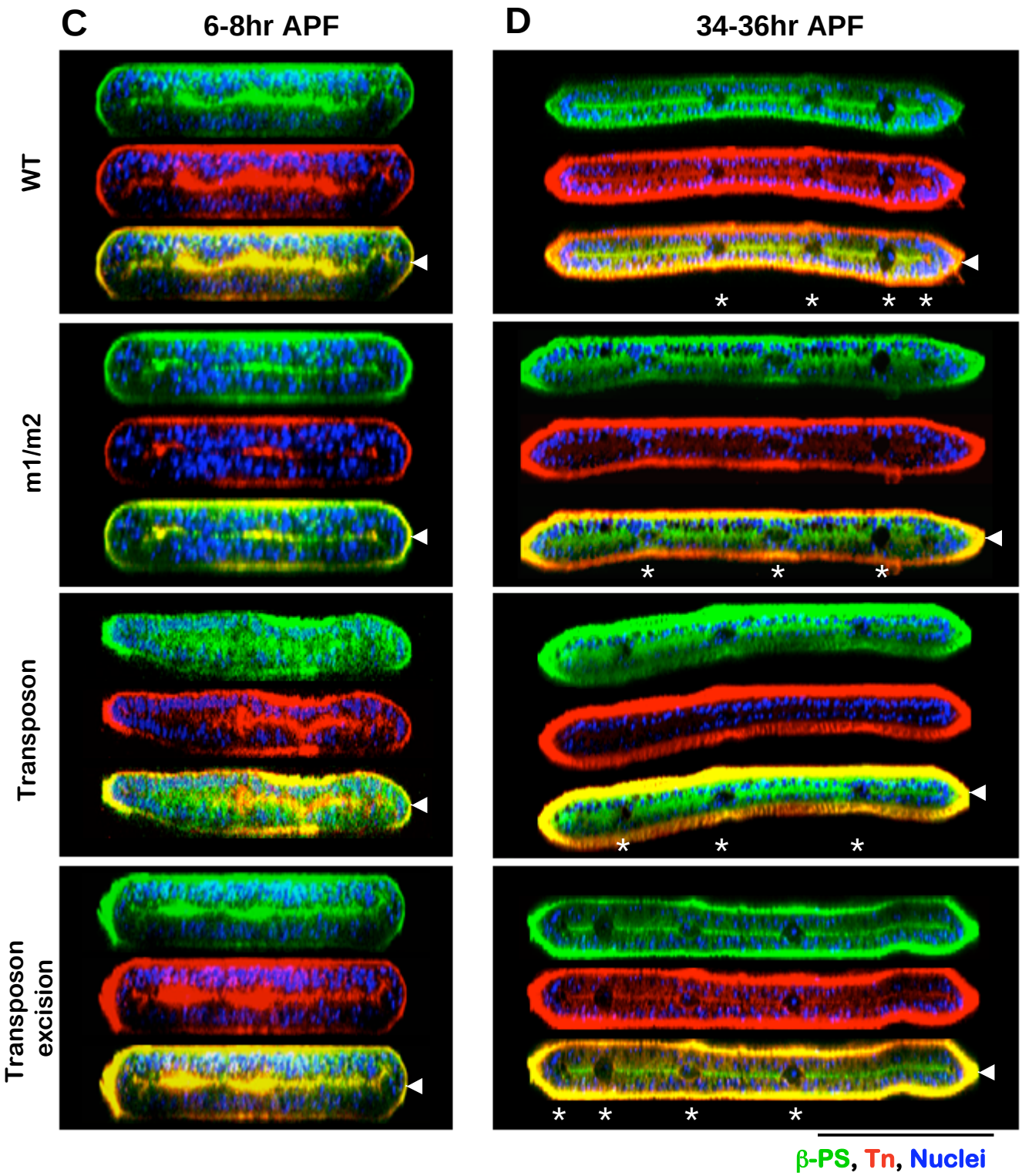

Fig.4

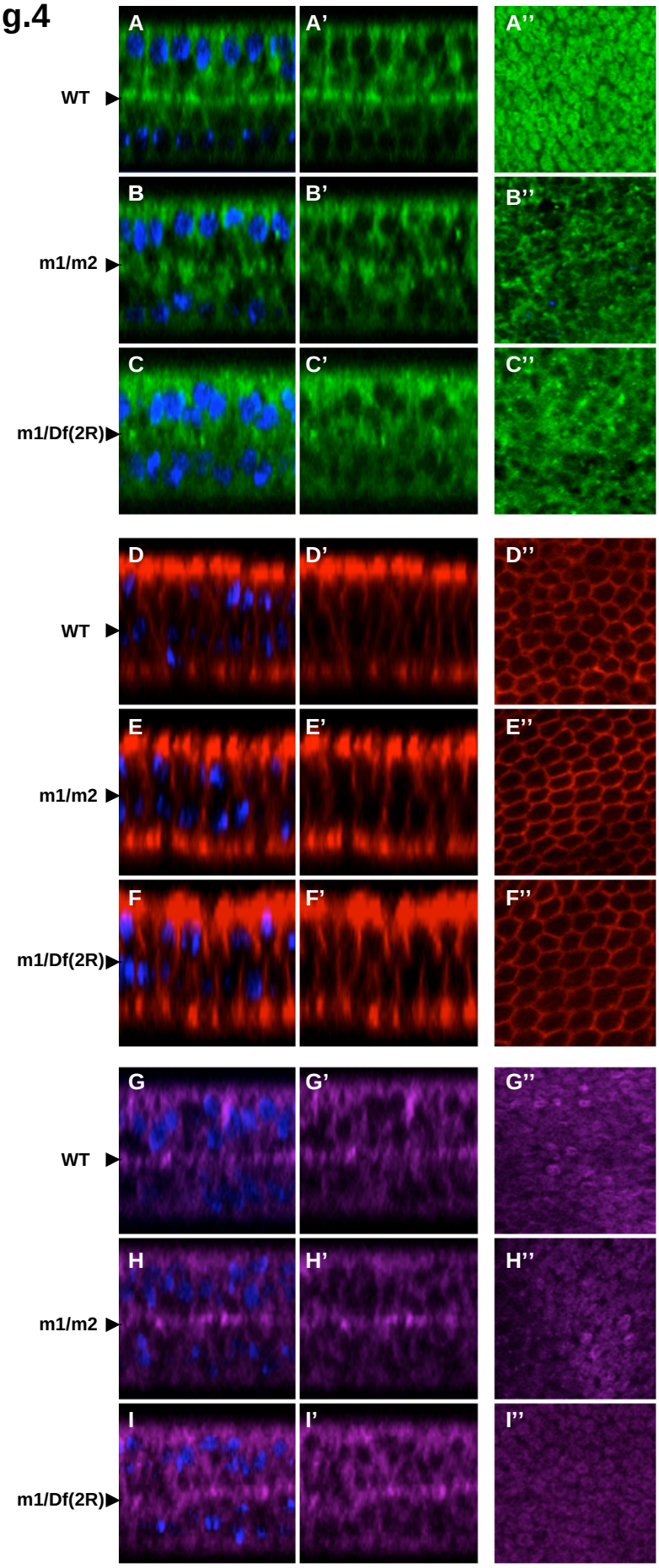

Fig. 5

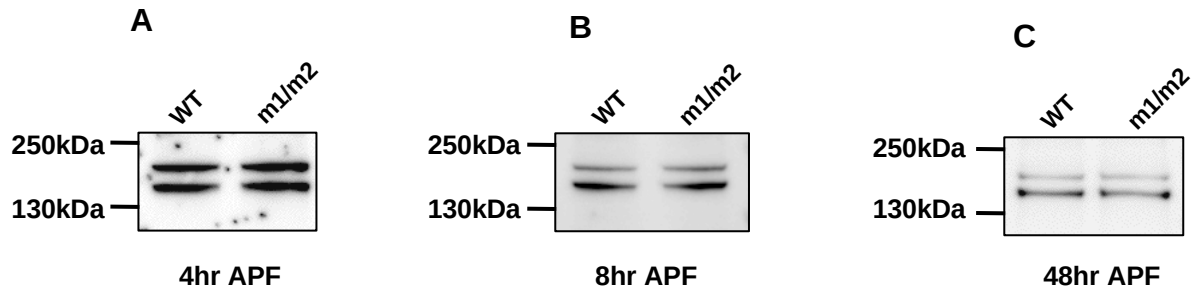

Fig.6

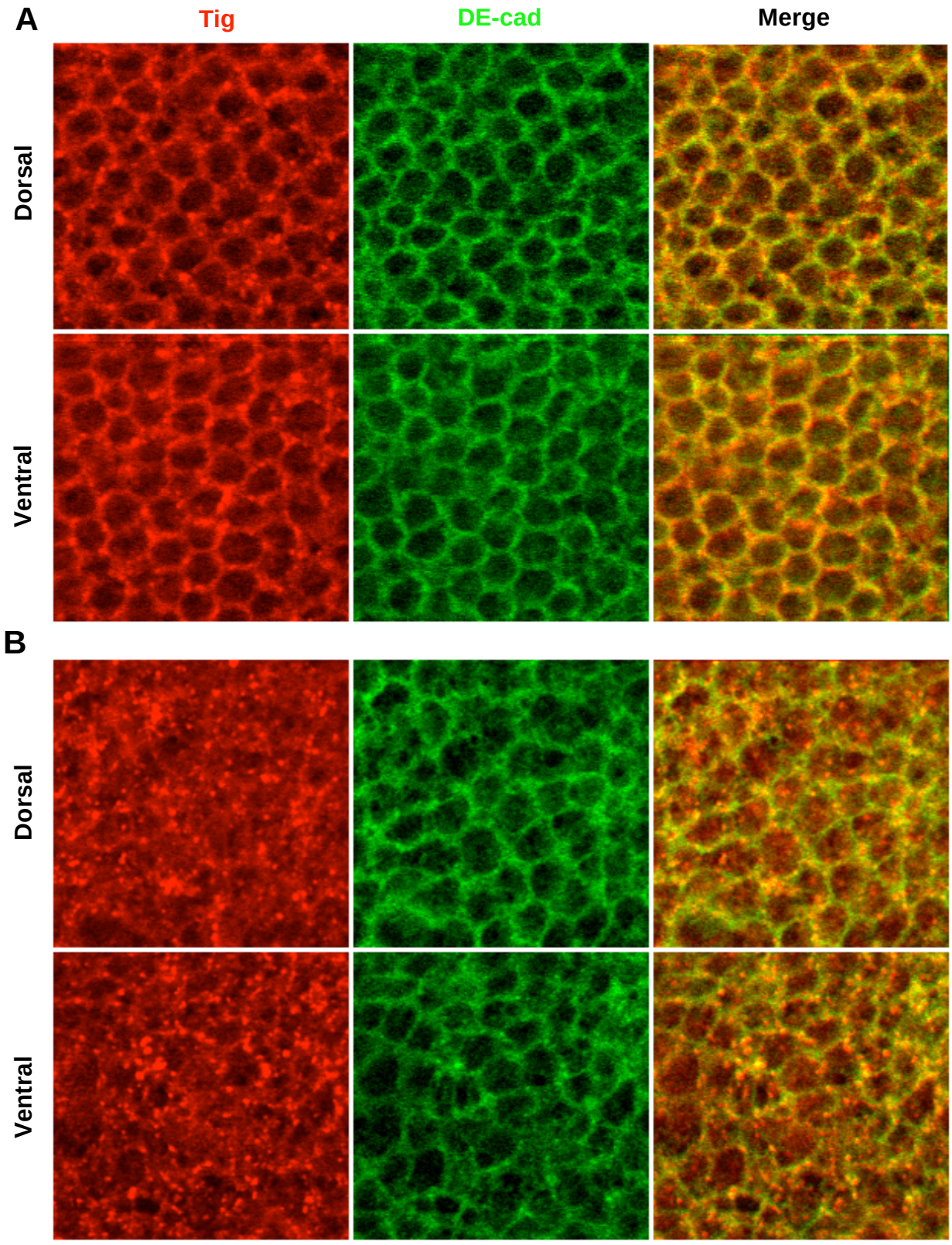

Fig.7

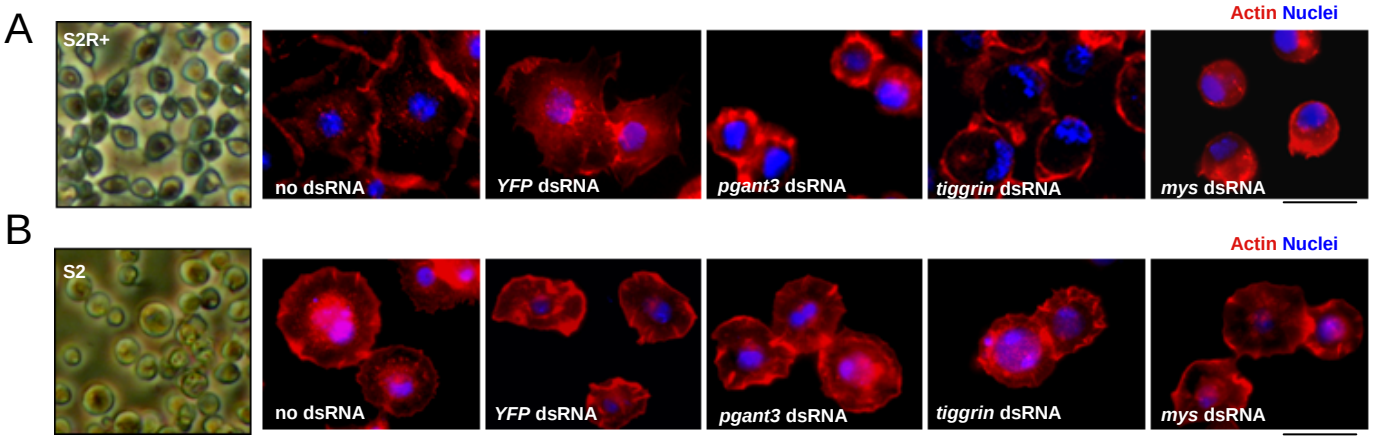

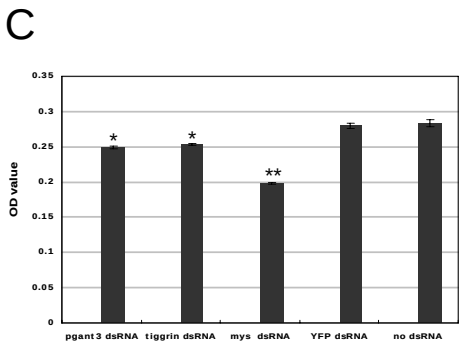

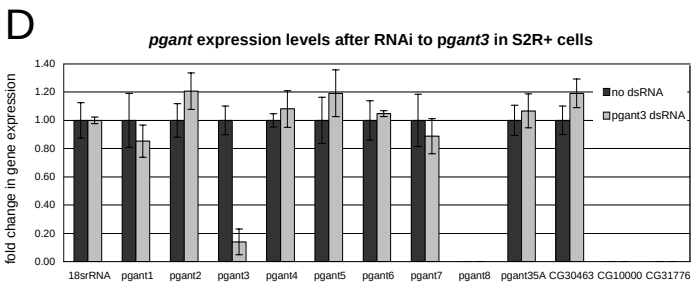

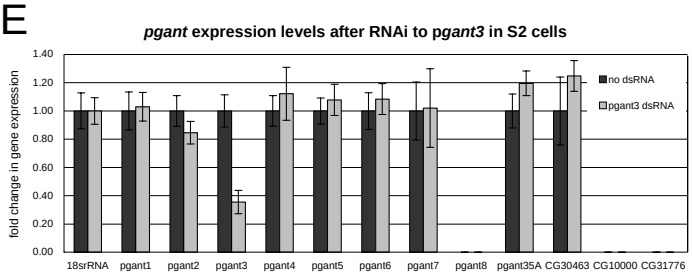

Table I. Frequency of wing blistering observed in *pgant3* mutants

Genotype	% Blistered*	n
pgant3^{m1}/+	**0**	**204**
pgant3^{m2}/+	**0**	**258**
pgant3^{c01318}/+	**0**	**107**
Def(2R) Exel6283/+	**0**	**232**
pgant3^{m1}/pgant3^{c01318}	**100**	**127**
pgant3^{m2}/pgant3^{c01318}	**100**	**132**
w; *pgant3^{m1}/ pgant3^{m2}*	**90**	**109**
pgant3^{c01318}/ pgant3^{c01318}	**95**	**129**
pgant3^{m1}/ Df(2R) Exel6283	**99**	**214**
pgant3^{m2}/ Df(2R) Exel6283	**100**	**198**

* (number of flies displaying blistered wings/total number of flies) X 100
n=total number of flies scored

Table II. Genetic interaction between *pgant3* and *if* (αPS2 integrin)

Genotype	% blistered*	n
w/Y; *pgant3^{m1}/+*	**0**	**129**
w/Y; *pgant3^{m2}/+*	**0**	**142**
***if^{3}*/Y; +/ +**	**17**	**87**
if^{3}*/Y; *pgant3^{m1}/+	**76**	**176**
if^{3}*/Y; *pgant3^{m2}/+	**52**	**125**

* (number of flies displaying blistered wings/total number of flies) X 100
n=total number of flies scored